Chapter 1

Introduction

In order to record high-definition digital video streams, both a capacity of more than 20 GB and a data transfer rate of more than 100 Mbps are required for optical data storage in the era of digital broadcasting and broadband networks. A shorter wavelength laser or multi-layer data disks can be used to increase the storage capacity. On the other hand, increasing the speed of the spindle motor can enhance the data transfer rate. In both approaches, it becomes more difficult for the pick-up to perform accurate tracking with high-speed disk rotation. Therefore, a high-speed, high-accuracy tracking control system employing a MEMS (Micro Electro-Mechanical System) micro-mirror is proposed to replace the traditional tracking servo with voice coil motor (VCM).

1.1 Optical data storage

The optical data storage industry has been growing rapidly with the progress of computers, multimedia, and network markets. Technologies for recording more information become increasingly demanded. There are several types of optical data storage for different applications, including read-only memory (ROM), write-once read-many (WORM) and rewritable disks. One example of ROM is the Compact Disk (CD) introduced in 1983. Digital Versatile Disk (DVD) is the successor to CD with higher density. Data are stored as embossed pits that induce changes in the reflected signals. The optical components in CD players are relatively simple, since the only function of the device is to read data through the plastic substrate. WORM

media are useful for customers who wish to record information permanently. Compared with CD players, more issues have to be addressed in order to focus more light energy on the recording layer during writing. The most popular example of WORM media is CD-R (CD-recordable). The organic dye material on the disk was locally modified by the focused laser beam, thereby leaving a location through which a change in reflectivity can be detected. Rewritable media differ from WORM in that data patterns can be erased, thus the storage layer can be re-used to record new data. In most cases, rewritable recorders are more complicated than WORM recorders because of additional complications in both writing or readout.**[1-2]** In practice, each type of storage presents its particular requirements to the optical system design. In the following sections, the discussion is focused on the tracking systems for future storage systems.

1.2 Position control systems

Regardless of particular optical technologies, it is important to keep the laser beam in focus on the desired track for reliable data storage and retrieval. The need for position control stems from the fact that the disks and drives have mechanical deviations both in the focusing and tracking directions. These deviations must be compensated for the system to operate properly. Radial runout is the term given to the eccentricity of the tracks on a disk while axial runout is defined as the deviation of the data surface along the optical axis. The performance of the focus and tracking servos has a direct impact on the maximum data transfer rate, data bit error rate (BER), and signal-to-noise ratio (SNR) during the read/write processes. Servo control systems are used to keep the closed loop position errors due to these runouts within tolerable limits, which are usually less than 0.1 um. The objective of this thesis

is to investigate a novel tracking method as well as to construct a reliable controller to optimize the system performance [3].

1.3 Tracking actuator in pick-up

Current major design challenge in optical data storage systems are slow data transfer rate and long access time compared to those of magnetic disk systems. These issues result from for relatively the massive dual mechanical actuators such as voice coil motors (VCM) or galvanomirrors.

1.3.1 Data transfer rate

A high-definition-television (HDTV) optical-disk camera recorder is desired in order to record HDTV programs more flexibly and efficiently. To this end, the new technology is being developed to achieve optical-disk performance equivalent to that of current camera recorders, i.e., high data rates of 100 Mbps or higher and large-recording-capacity capable of storing more than 60 min of a HDTV signal. High disk rotation speed is required to achieve a high data transfer rate. Together with the utilization of short-wavelength lasers and an objective lens with a high numerical aperture, the track pitch on the disk must also be reduced to enlarge the recording capacity as shown in Table 1.1. Optical disks have a radial run-out in the range of 50 um to approximately 100 um peak-to-peak, which is the primary cause of track eccentricity. The tracking servo system must follow the track to keep the residual tracking error below the tolerance. Therefore, a fast and precise tracking servo system is indispensable for recording and retrieving data with high data transfer rate from a large capacity optical disk.

Table 1.1 Comparison between CD-ROM and DVD-ROM

	CD-ROM	DVD-ROM
Spindle speed (rpm)	230~6000	580~5000
1st Resonance Freq. (Hz) (tracking actuator)	60	95
Bandwidth for tracking actuator -3dB point(Hz)	<100	<200
Maximum data transfer rate (Mbps)	48	100

1.3.2 Access time [4-6]

Nowadays, all kinds of affordable and removable storage media are currently available that have the additional capacity of high speed accessing. CD and DVD historically stem from the consumer industry where access time is not a critical factor since the audio and video data are predominantly read sequentially rather than randomly. However, there is an increasing demand in both consumer and the computer markets for fast random-access optical drivers. Traditional optical heads are considerably larger and heavier than the magnetic heads in hard disk drives (HDD). Thus, the access time of the optical drivers is larger than that of HDD. To achieve short access time (<100 ms) and high accelerations (>500 m/s^2), the weight of the moving part in an optical head needs to be reduced drastically by developing miniaturized head component. These components are expected to reduce the cost, size, and weight of the opto-mechanical structure, making the device more competitive in terms of price and performance.

1.4 Head miniaturization

Improvement of advanced pickups includes miniaturization, integration, and parallel processing (multiple beams). These approaches can reduce the cost, size, and weight of the opto-mechanical structures, making the devices more competitive in terms of price and performance.

Micro-electro-mechanical-systems (MEMS) technology [7-9]

With the tremendous progress in semiconductor electronics field, many efforts have been made to extend the idea of microintegration to other applications such as, particularly, mechanics and optics to boost the performance. Such efforts are interesting for areas and applications where electronics, mechanics, and optics overlap and eventually lead to the development of the Micro-Mechanical-Systems (MEMS).

Recently, the interest is raised in the monolithic integration of optical pickup by MEMS technology. The integration not only reduces the assembly cost by eliminating bulk optical elements but also enhances the device performance.

Issues in new head design include miniaturization, integration, and multiple beams. Each of these topics is a subject of active research. Here we only discuss the possible characteristics of the optical pickup fabricated by MEMS technology, such as the focused spot size, focusing/tracking servo operation, and the resolution of readout. The schemes of the integrated optical pickup were introduced:

Free-space optical bench by surface micromachining techniques [10]

The silicon surface micromachining is proposed by M. C. Wu *et al*. A Si substrate serves as a micro-optical bench on which three dimensional optical elements, such as

micro-sensors, micro-mirrors and actuators are monolithically fabricated. All configurations of this technology are the same with the conventional pickup but on an extremely tiny size. The schematic drawing of the pickup is shown in Fig. 1-1. The NA of the focusing micro Fresnel lens was measured to be about 0.17. In this structure, fine optical alignment (< 0.1 μm) and dynamic tracking can be achieved by on-chip microactuators with electronic driving. A comparison of this approach for integrated-optic pickup device is presented in Table 1-2.

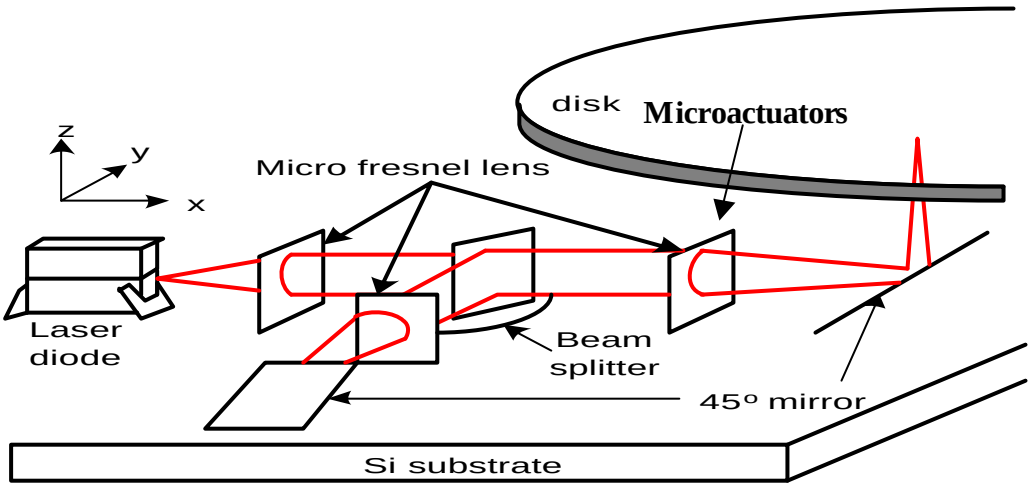

Fig. 1-1 Optical module structure.

Table 1-2 Pros and Cons of free-space integrated optic disk pickup

Pros	Cons
Free-space optical bench using surface-micromachining technique	
1.**Three dimension dynamic calibration** **2. Free space can perform optical imaging and generate diffraction- limited focused spot** **3.Simple mechanical structure and electric-static actuation are easily driven with high bandwidth**	**1. Cumbersome fabrication process** **2.With high driving voltage**

With these advantages, the MEMS technology has been proposed to make the head smaller and lighter for fast access, direct overwriting and high data transfer rate.

1.5 Objective of this dissertation

To achieve higher access speed and data transfer rate, it is desirable to replace low-bandwidth components with high-bandwidth ones. At the same time, to reduce the size and weight of pick-up can enhance access speed. Hence the main goal of this research work is to develop a new-structure pickup module, which combines a high-bandwidth tracking mirror by MEMS technology. The major purpose of the tracking mirror is to increase the bandwidth of the tracking system for high access speed and data transfer rate. Moreover, the tiny size of the tracking mirror can facilitate the miniature requirement for future pick-up design. In this thesis, the use of a high bandwidth and small size MEMS mirror will be discussed and demonstrated to improve track following and track access performance in optical storage system.

1.6 Organization of this dissertation

The dissertation is organized as follows: The theoretical background of tracking mirror is presented in Chapter 2. A historical overview including focusing and tracking technologies is given. Furthermore, the tracking mirror is employed to build an optical system model, which discusses the relation between aberration and mirror's tilt. In Chapter3, Some measurements of the mirror dynamic characteristics are introduced and the experimental results of tracking mirror are demonstrated. In Chapter 4, system identification of the tracking mirror is discussed. A control strategy is proposed and simulated by MATLAB. Preliminary optical system design and measurement are demonstrated in Chapter 5. Discussion and recommendation for the future work are given in Chapter 6.

Chapter 2

Micro-mirror tracking system

Micro Electro-Mechanical System (MEMS) technology is an attractive technology because micro-sized devices can be fabricated to operate in high resonance frequency. Therefore, using a MEMS tracking mirror as the fine actuator is proposed for high-precision tracking actuator. In the following sections, the basic principles of tracking system are presented. Moreover, the relative knowledge including tracking servo, micro-mirror and the simulation results between aberration and tilt angle were discussed.

2.1 Optical focusing/tracking servo

During all read/write/erase operations, it is important to keep the spot in focus and follow the track in the radial direction. In practice, however, the axial and radial runouts of optical disks, as shown in Fig. 2-1, are two to three orders of magnitude higher than the allowable focusing/tracking errors. Typical values of the relationship between the focused spot and runout are presented in Table 2-1. Therefore, the objective mounted on the actuator (usually a voice coil) must be controlled to follow the runouts in real time. The frequency responses of these feedback systems (also referred to as servo systems) are used with a bandwidth of several kHz.

Table 2-1 Typical value of axial and radial runout in the disk

Combined axial runout (Dt): 50-200 mm (~ 100X depth of focus Dz)
Reasons: 1. Substrate thickness variation **2. Disk tilt** **3. Spindle wobbles** **4. Vibration**
Combined radial runout (Dr): 30-100 mm (~ 100X focused spot size Dx)
Reasons: 1. Decent-ration of the tracks of a disk **2. Spindle wobbles**

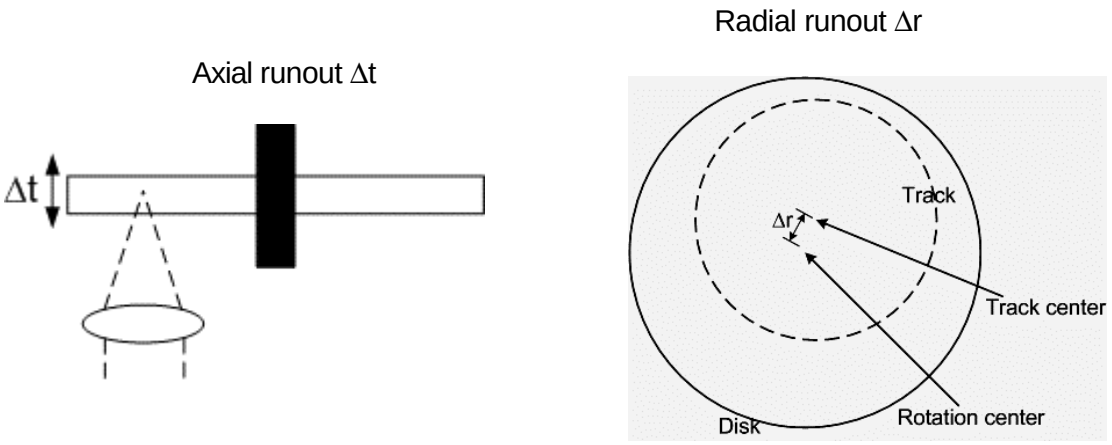

Fig. 2-1 Axial runout and radial runout of disk

The focusing and tracking error detection used in MEMS tracking system were astigmatic and push-pull methods introduced below.

Focus error detection (Astigmatic method)

The focus sensor in an optical pickup must detect disk defocus with the sensitive resolution in terms of detector photocurrent (mA/μm) and low noise ($<10^{-3}$μm-RMS) for servo electronics. Various methods can be employed to derive the

focus error signal (FES) in the opto-mechanical system, as best they can, while minimizing complexity.

Depending on the convergent angle of the reflected beam, astigmatism is introduced with astigmatic lens that generates two focal lines in the sagittal and tangential planes along the optical axis, as shown in Fig. 2-2. Meanwhile, the push-pull tracking signals are also available in the far field of the beam and can be detected by the same quadrant detector. Although this method has lower sensitivity and a higher level of focus-to-tracking optical crosstalk, its acquisition range is larger than that of the Foucault knife-edge method.

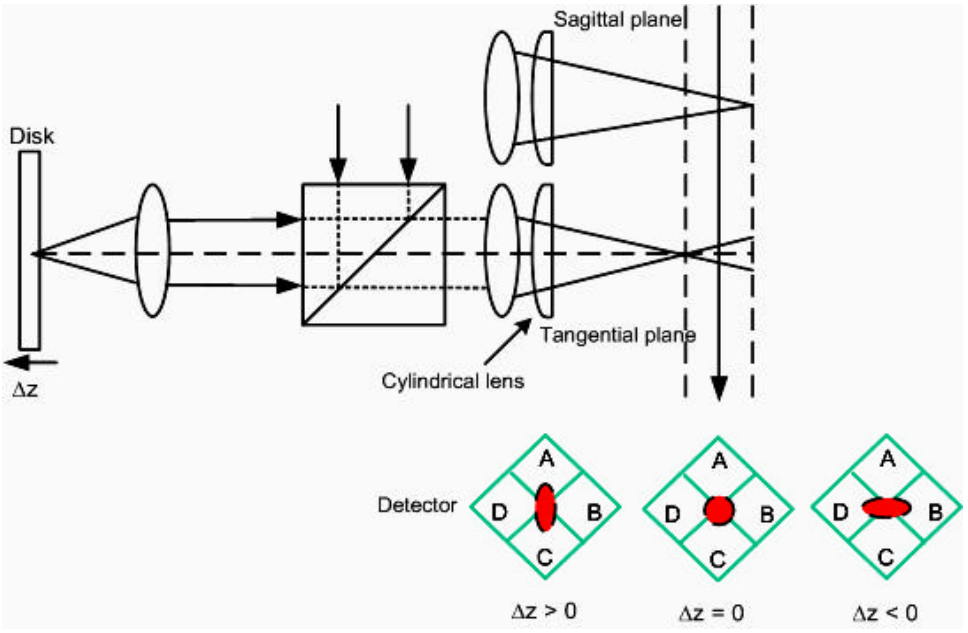

Fig. 2-2 Astigmatic focus error detection method.

Tracking error detection (Push-Pull method)

The tracking error signal (TES) of push-pull method is derived in most pickups from the far field pattern diffracted symmetrically from the two edges of the track. As soon as the spot moves away from the track center, the symmetry of the far field

pattern breaks down and the light distribution tends to shift to one side or the other. A split photo-detector placed in the path of the reflected light can therefore sense the relative position of the spot and provide the appropriate feedback signal as shown in Fig. 2-3. Tracking error sensing is achieved with this method (for continuous tracking) [11]. When combined with appropriate closed-loop servos, it can hold tracking errors to less than 0.1 μm.

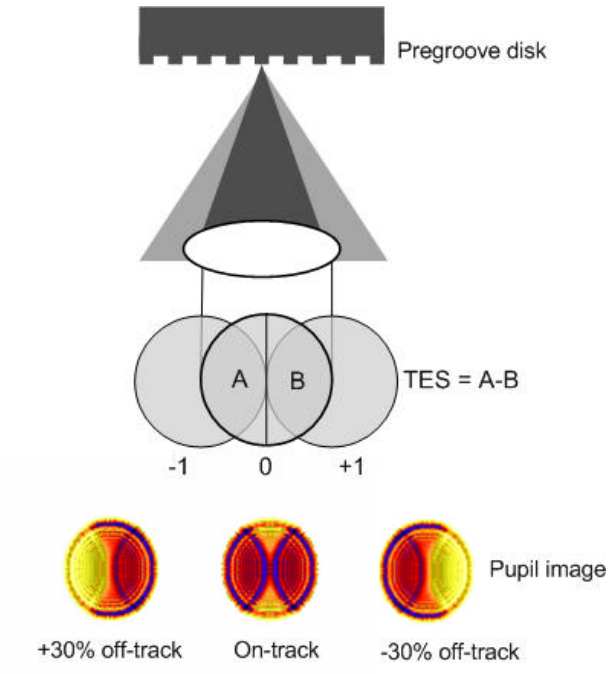

Fig. 2-3 Reflected zeroth-order and diffracted light interferes to yield the push-pull track error signal.

2.2 Tracking following literature survey

To achieve a high-speed access mechanism, **Matsushita [12] and IBM [13]** developed a drive configuration with a high-sensitivity galvanomirror mounted on a nonmovable part of the system for improving the actuator performance. The

galvanomirror was used as the fine-tracking actuator, which mounted on the separated part of the system can interact less with the vibration modes of the coarse actuator than placed directly on the coarse actuator.

For improving both the track access time and data rate for future high performance optical disk drives, **C M U [14]** reported on the use of an electro-optic (EO) scanner with the bandwidth of 200 kHz as tracking following actuator. A fine tracking experiment has been demonstrated using an EO actuator to improve tracking performance.

Meanwhile, Fujitsu **[15]** proposed a dual-stage tracking control system. In their scheme, a MEMS tracking mirror was used as a fine actuator mounted on a coarse positioner without inducing any undesirable mechanical resonance. Compared to ordinary two-axis lens actuator, this MEMs tracking mirror can contribute to a higher bandwidth of the tracking-following control. The tracking error was demonstrated experimentally of less than 10 nm in this method.

2.3 Introduction to MEMS tracking system

Compared to galvano mirror, the MEMS mirror can be mass-produced by photolithography and this is expected to reduce production costs. Because MEMS mirror is smaller and lighter, it can be mounted on a coarse actuator without adversely affecting the fast motion of the actuator. Moreover, compared to an ordinary voice coil actuator, the MEMS mirror has higher mechanical resonance because of its simple mechanical structure and electrostatic actuation. Therefore, using micro-mirror as tracking device can contribute to a higher bandwidth of tracking system in high-density and fast-speed optical disk drives.

2.4 Specification of the micro-mirror

The commercially available micro-mirror fabricated by MEMS Optical **[16]** is the product that with steady dynamic features and quality. We selected this device as the tracking mirror because of its high reflectivity and high resonant frequency. The schematic of the mirror is shown in Fig. 2-4 and its brief specification of the micro-mirror is shown in Table 2-2. The mirror is approximately octagonal, 520 microns across, with a 5-micron perimeter around the gold coating. Six bond pads are provided, four for the bottom electrodes and two ground pads. Each bond pad is roughly 200 microns square.

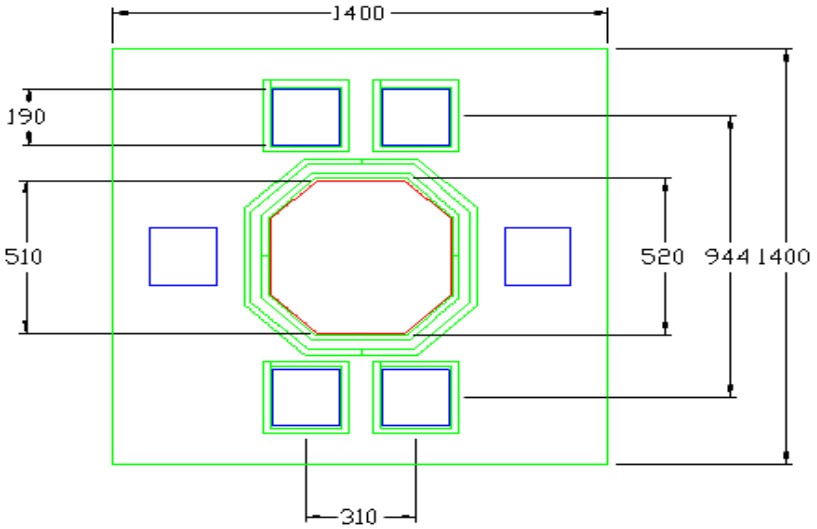

Fig. 2-4 Dimensions of mirror (um)

Table 2-2 the brief specification of micro-mirror

Mirror Size	**520μm across**
Reflective area	**510μm across**
Shape	**Octagonal**
Surface Roughness (rms)	**< 25 nm**
Surface reflectivity	**>95% at 630nm (gold)**
Drive voltage	**0~110 Volts**
Maximum tilt angle	**+/- 3° mechanical**
Resonant rotation frequency	**Outer axis 1.3 kHz, inner axis 1.8 kHz**
Radius of Curvature	**> 0.4 meters**

2.5 Micro mirror tracking system

2.5.1 Configuration of optical system

A tracking system with a larger working bandwidth can partly reduce the access time. The optical test system with a MEMS tracking mirror as a large bandwidth fine actuator is shown in Fig. 2-5. In this system, only the objective lens moves during focusing; the other components are fixed. The fixed part includes a tracking mirror which is mounted at 45^{o} to the optical axis. The conventional astigmatic technique and push-pull detection are used for FES and radial tracking error signal generation, respectively. On the disk surface, the beam spot is controlled by the tracking mirror and focused by the objective lens.

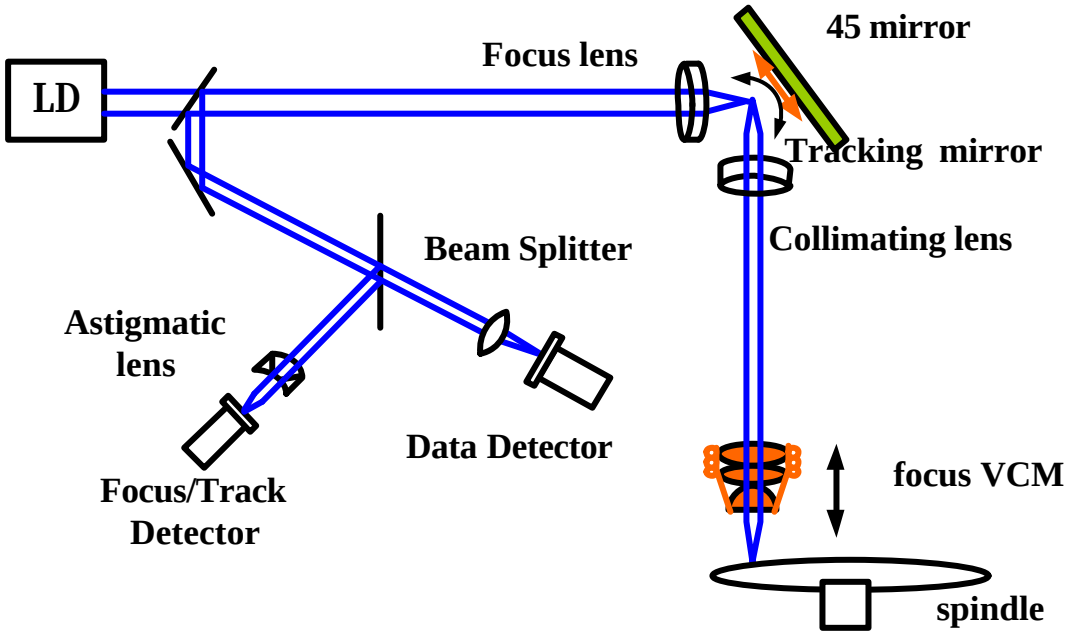

Fig.2-5 Micro-mirror tracking system

Since the diameter of micro-mirror is 520 um, the laser spot focused on the mirror need to be smaller than the dimension of mirror's surface. According to the diffraction theory, the minimum focused spot (full-width at half-maximum) is about

Spot size= 0.6λ/NA.

Where λ and NA are the laser wavelength and the numerical aperture of the objective lens, respectively. The twin relay lens of 0.1 NA are configured in tracking system. One relay-lens is used to focus laser spot small to 4um; while the other one is used to collimate the focused light. The laser beam passing through objective lens with 0.6 NA is focused on the disk.

The laser spot position in the tracking system was controlled by the mirror's tilt as shown in Fig. 2-6.The movement X1 of the focus actuator, which focuses the laser beam on the disc surface, is vertical. The spot displacement X2 is caused by the mirror's scanning. As these two movements (X1 and X2) are orthogonal to each other, they are analyzed separately. However, the tilt of the incident beam due to the mirror's scanning may also result in truncation of the collimated beam and optical aberration. Therefore, the fine stage stroke should be limited on micro-mirror to prevent optical distortion. Moreover, the tracking error signal can be generated by an optical sensor based on push-pull tracking method.

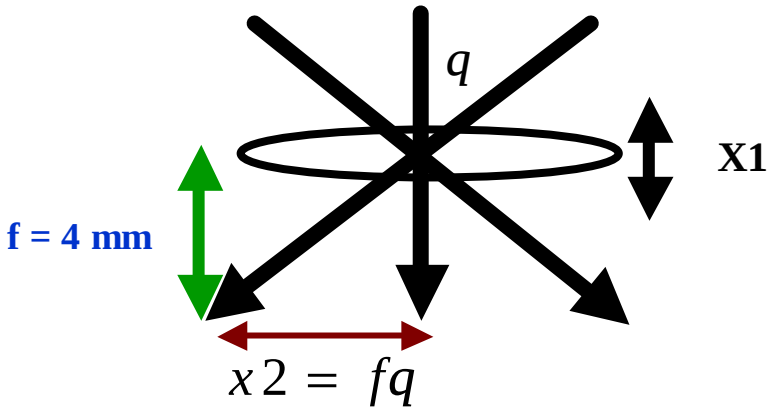

Fig.2-6 laser spot position

2.5.2 Aberration

The prerequisite for achieving a diffraction-limited spot is that the various aberration terms of the lens system should be small in a tolerable range. The detector can also obtain correct signals with tolerated aberration. Therefore, since the tracking displacement X2 comes from the mirror's tilt, it is important to consider the relation between the aberration and tilt in the system. According to the DVD specification, a 0.6-NA objective lens is used to read 0.4 μm shortest pit length and 0.74 μm track pitch. Lenses with large NA in this situation, however, are sensitive to coma aberration caused by mirror's tilt. Therefore, the tilt range of mirror is restricted to prevent the system working outside the detectable field.

By using the ZMAX simulation tool, the relation between aberration and mirror's tilt angle can be analyzed. Based on DVD standard, the allowed leaning angle of micro-mirror can be defined following the simulation results. The layout of the micro-mirror tracking system shown in Fig. 2-7 is based on the DVD specification, such as 660nm wavelength, 0.6-NA objective lens and 0.6 mm polycarbonate.

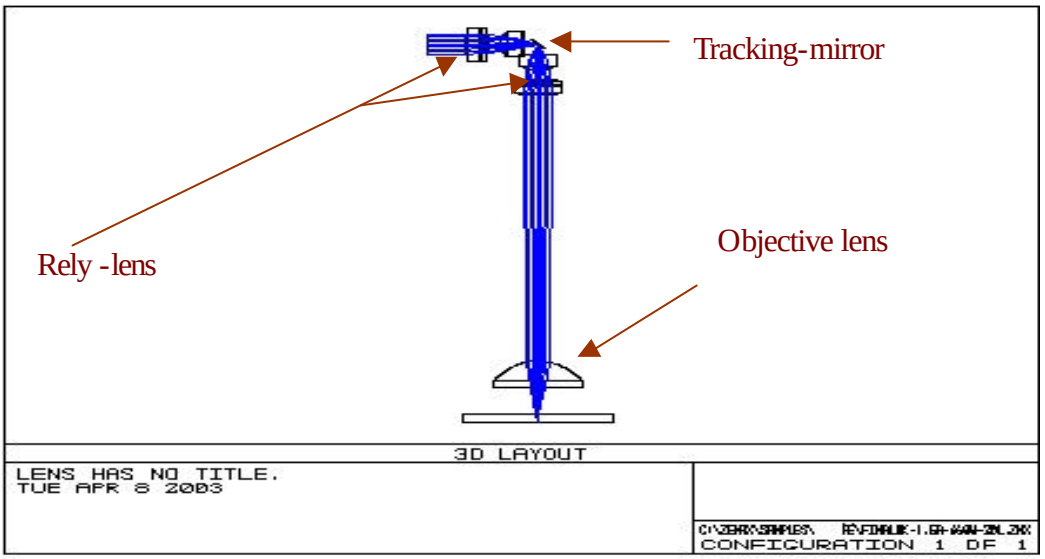

Fig.2-7 3D layout of tracking system

The spot diagram of the beam focused on the disk in the system without mirror tilting is shown in Fig. 2-8(a), whose RMS radius 1.15 l is larger than the radius of diffraction limitation, (0.6λ/NA) equal to l for NA=0.6. On the other hand, the value of optical path difference simulated can be used to determine the quality of optical system shown in Fig. 2-8(b).

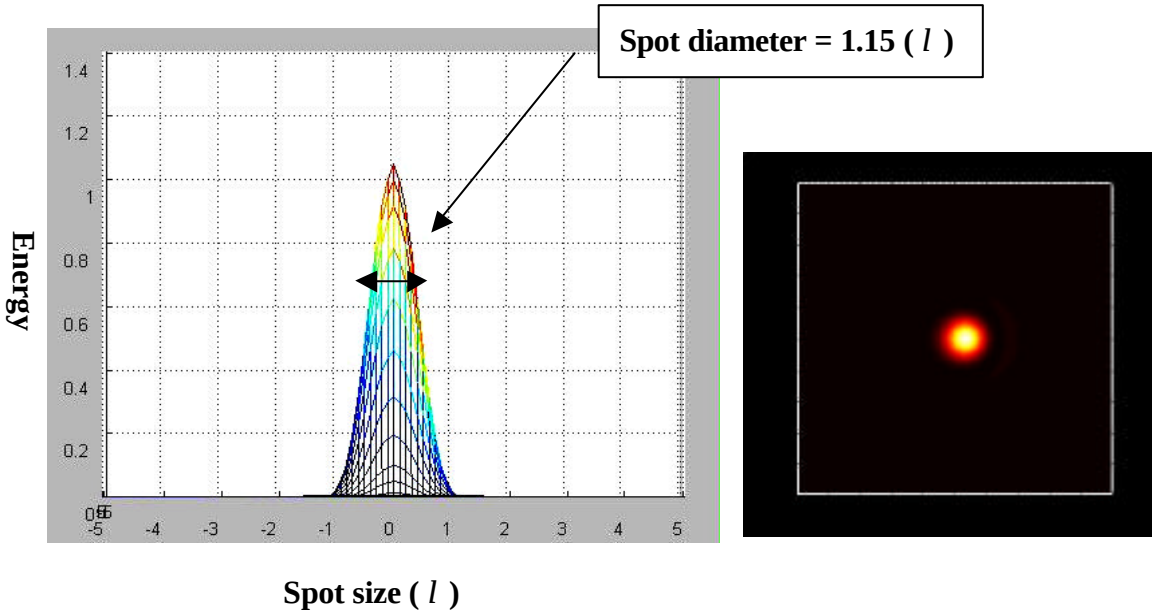

Fig. 2-8 (a) The spot diagram of tracking system without tilting

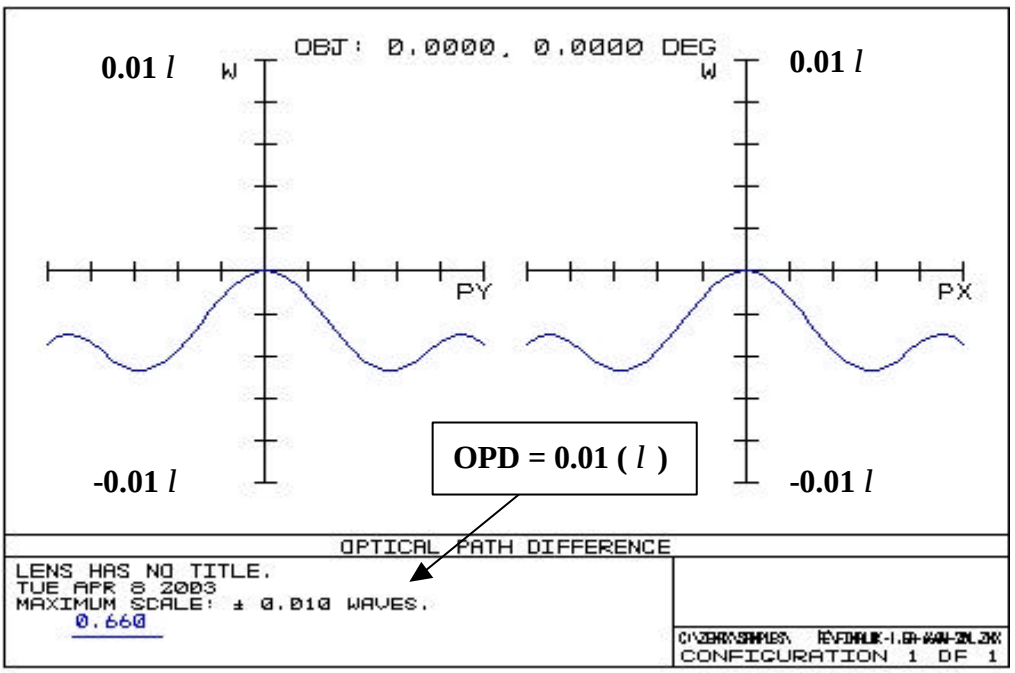

Fig. 2-8(b) The OPD of tracking system without tilting

Based on the DVD optical design standard, the max aberration is allowable as the value of OPD below 0.06 l based on DVD pick-up design standard. The OPD below 0.06 l means 80% energy are still within the spot. Therefore, the results of optical simulation to define the reliable tilt angle of tracking mirror are examined and evaluated in tracking system. These data calculated with ZMAX and DIFFRACT simulation tool are shown in Table 2-3, which clearly direct that the maximum of tolerated angle of tracking mirror was ± 1 degree. The spot diagram of tracking system with 1^{o} tilt was shown in Fig. 2-9.

Table 2-3 the relation between OPD and tilt angle

Spot pattern

Tilt (degree)	0	0.5	1	1.5	2
Spot size (λ)	1.15	1.28	1.47	1.72	2.1
Optical path difference(λ)	0.01	0.02	0.06	0.08	0.1

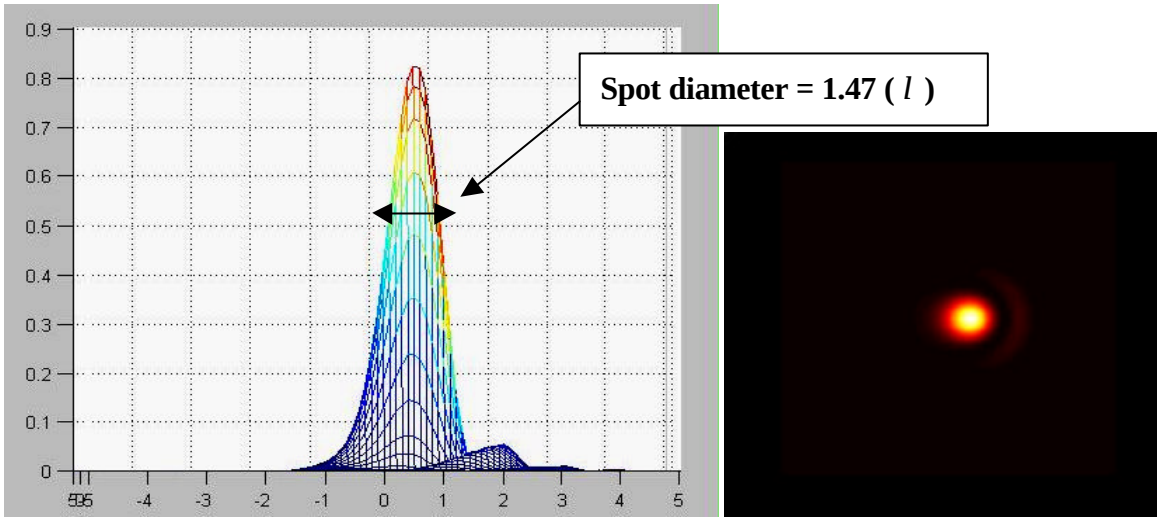

Fig.2-9The spot diagram of tracking system with 1^{o} tilt

2.6 Summary

The allowable tilt angle of micro-mirror above tracking system was obtained from the simulation in ZMAX. The micro-mirror, involved in tracking system for improving access time, was discussed with the simulation of the optical quality. With these results, however, only the static characteristics can be analyzed, which was not enough to estimate the dynamic behavior of the tracking mirror. In the Chapter 3, two dynamic measurements are performed to characterize the mirror's dynamic features.

Chapter 3

Dynamics of micro-mirror

In order to improve the performance of the tracking system, an appropriate controller is needed for the micro-mirror. Because the controller design is based on the dynamic features of the micro-mirror, a dynamics measurement of the micro-mirror is required. In this chapter, two dynamic characterization measurements of the micro-mirror, one with CCD sensing array and the other with a (dynamic system analyzer) DSA, are presented. The dynamic features, such as temporal response, bandwidth, and scanning angle, etc were measured and calculated from the experiment. By analyzing these features, the physical model of the micro-mirror was identified.

3.1 CCD dynamic measurement system [17]

3.1.1 Architecture of CCD measuring system

The architecture of the CCD measurement system is shown in Fig. 3-1. It is composed of four parts:

(1) The driving platform provides the necessary driving signals to the micro-mirror by using a function generator.

(2) The optical system is designed to provide adequate light source for measurement.

(3) The Altera CPLD driving and processing circuits supply driving signals to the

CCD and calculate the spot size and position.

(4) A computer catches and analyzes information from the CCD circuit with interrupting signals.

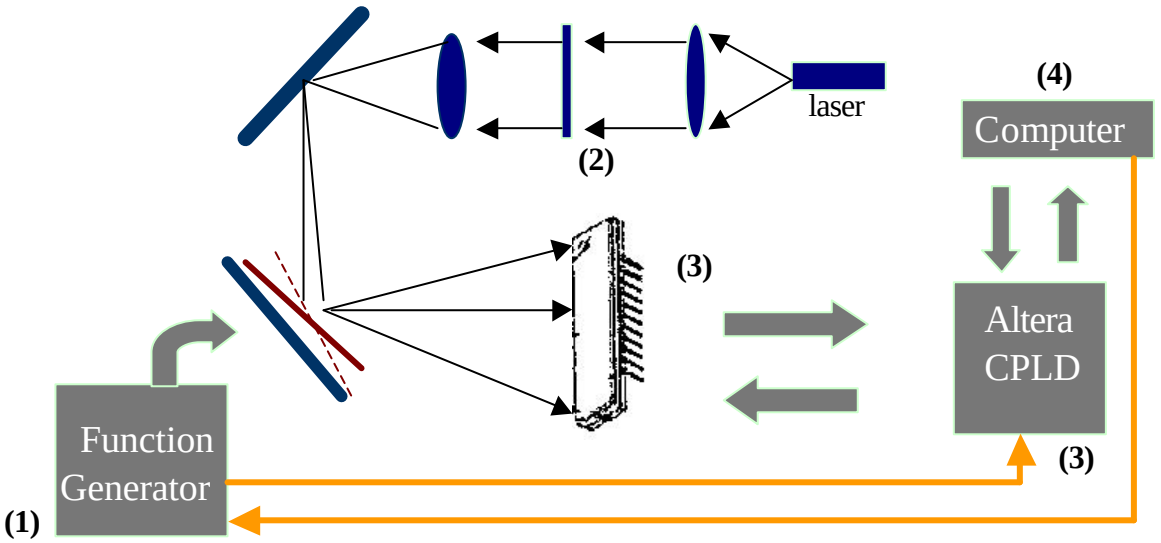

Fig. 3-1 Architecture of CCD measurement system

3.1.2 Driving platform

MEMS micro-mirror is driven by electrostatic force. In this approach, the mirror is usually actuated with high voltage and needs a special voltage amplifying circuit. In our experiment, the driving electronics was provided by MEMS Optical. A photo of the two-axis tilt mirror chip is shown in Fig. 3-2. The mirror was removed to illustrate the electrode configuration. Actuation is achieved by applying a drive voltage to the desired electrode. The mirror plate is electrically grounded and bonding pads are provided to drive on the sides of the chip shown in Fig. 3-3.

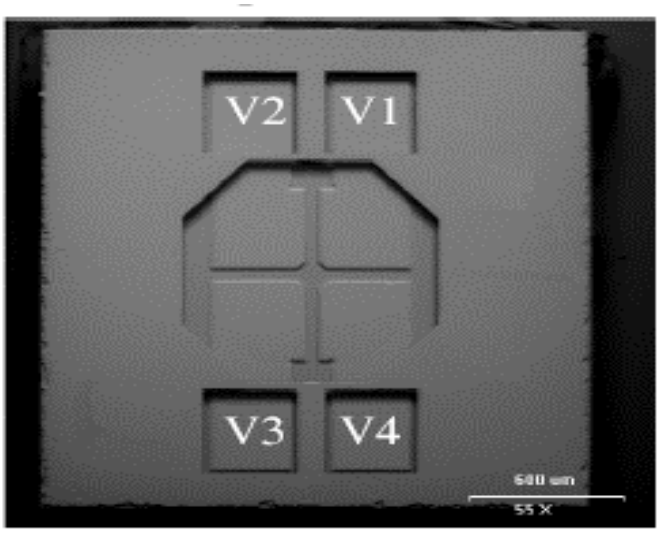

Fig. 3-2 Electrode pattern and numbering.

In order to make the voltage-deflection responses more linear, MEMS Optical recommends that the drive signals be generated according to following equations:

$$V_1 = V_{bias} + k\ (+ V_x - V_y)$$
$$V_2 = V_{bias} + k\ (+ V_x + V_y)$$
$$V_3 = V_{bias} + k\ (- V_x + V_y)$$
$$V_4 = V_{bias} + k\ (- V_x - V_y),$$

where k is the driving electronics gain, which is equal to 10.5 and V_{bias} is from 25V to 55V for drive electronics.

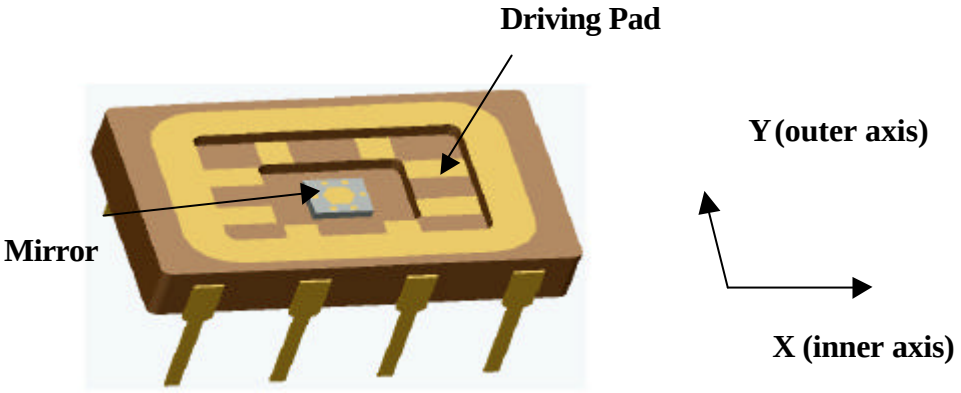

Fig. 3-3 Inner and outer axis of micro-mirror

The orientation of the chip is shown in Fig. 3-3, the inner axis of hinges lies in the x-plane and the outer axis lies in the y-plane. Square waveforms with different frequencies from the function generator are applied to the micro-mirror as the referring signals Vin. By comparing referring signals Vin with the scanning results from the CCD IC, the dynamic features of mirror could be obtained.

3.1.3 Optical system

The optical system for measurement is similar to the tracking system described in the previous chapter, but another 45 degree folding-mirror is added to accommodate for the limited space on the experimental platform. By using the same lens configuration, we can measure the real spot motion in the tracking system. Rely-lens can focus the spot to less than 100um to fit the demands of surface area in micro-mirror. The optical system of dynamic measurement is shown in Fig. 3-4.

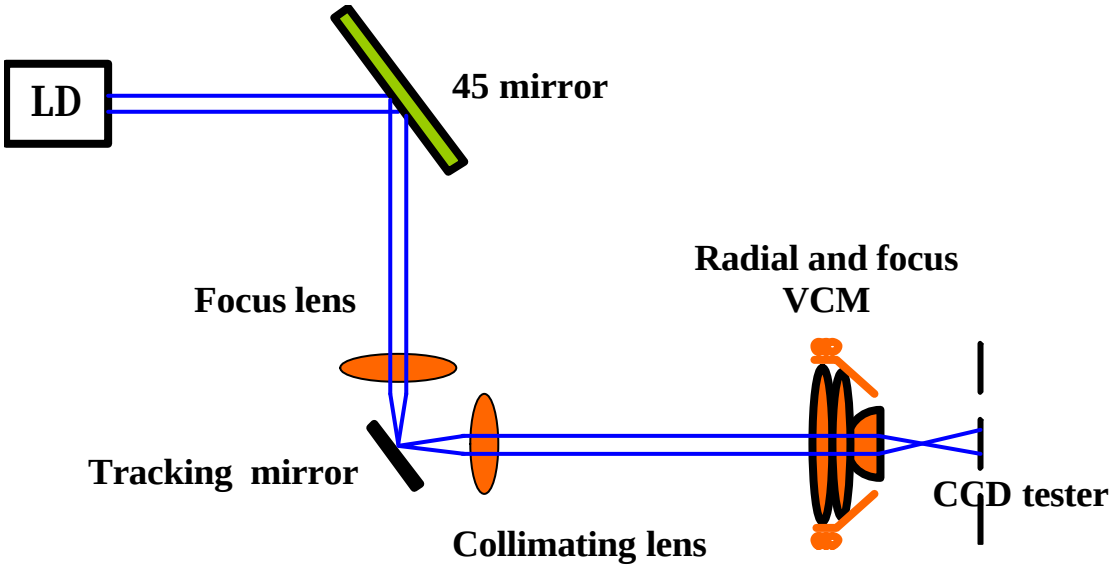

Fig. 3-4 The optical system of dynamic measurement

3.1.4 CCD and driving/processing circuits

The access time and the bandwidth of the storage system are limited by the dynamic characteristics of the actuators. An actuator with higher bandwidth and easy driving method not only can reduce the cost of controller but also increase the access speed. In the micro-mirror tracking system, the micro mirror is used to replace the voice coil motor due to its higher bandwidth and smaller size. But its dynamic features such as temporal response, bandwidth, and scanning angle need to be examined before designing appropriate controllers. An optical measurement system based on a linear CCD array was constructed for this purpose.

The system uses a linear CCD sensing IC (ILX503A) **[18]** produced by SONY with appropriate driving and signal process circuits. The specification of this CCD is shown in Table 3-1 and the architecture of the device is illustrated in Fig. 3-5.

Table 3-1 Specification of CCD

Features

- Number of effective pixels: 2048 pixels
- Pixel size: 14μm × 14μm (14μm pitch)
- Built-in timing generator and clock-drivers
- Ultra low lag
- Maximum clock frequency: 5MHz

Absolute Maximum Ratings

• Supply voltage	V_{DD1}	11	V
	V_{DD2}	6	V
• Operating temperature		–10 to +55	°C
• Storage temperature		–30 to +80	°C

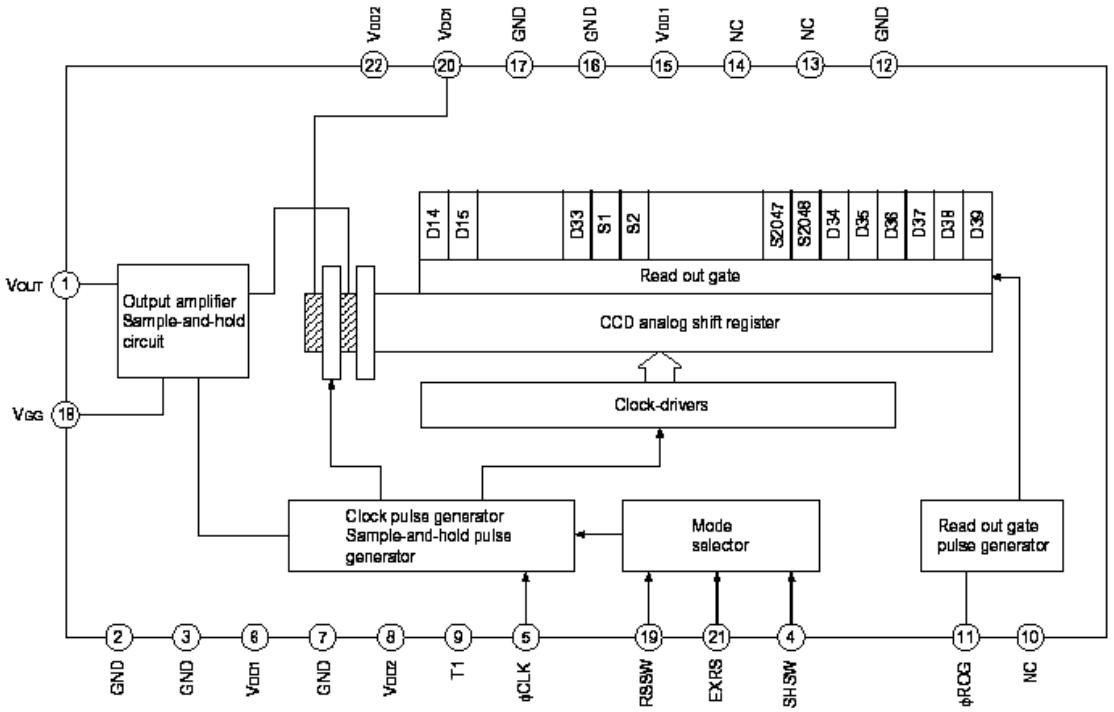

Fig. 3-5 Architecture of CCD IC

The pixel size of the CCD array is 14um X 14um. The detector wavelength is sensitive to visible wavelength, which is compatible to the DVD standard. From Fig. 3-5, the CCD analog shift register is driven by an outside clock signal f CLK and the CCD sensing data are gated by an outside signal f ROG. Based on the option of the Mode-selector, CCD can be operated in different modes (internal or external mode). In our experiments, the internal RS mode is used. Its clock timing diagram is shown in ref. Plot A-1. The operation of the CCD driving and processing circuits is described as follows:

(1) **Driving circuits**

VHDL codes with MAX-plus2 software are used to configure the Altera

10K10LC84-4 CPLD to generate driving signals fCLK and fROG.

(2) **Signals processing circuits**

In order to achieve the dynamic features of micro-mirror, the output signals from CCD are necessarily analyzed here. The drop of output signal V_{out} out from CCD array is proportional to the intensity of light at each pixel. If the CCD array does not receive light, the output signal V_{out} is the same as the input signal fCLK; on the other hand, if it receives light, the output signal V_{out} will have a voltage drop proportional to the intensity of light. For example, if the voltage of V_{out} has a drop from the 700th pixel to the 800th pixel, it can be inferred that CCD detect a spot with a width of 1400 um (100 X 14um) and the position of the spot is from 700th to 800th pixel.

The Altera FLEX10KLC84-4 CPLD **[19]** that processes the output signals V_{out} from CCD sensor is shown in Fig. 3-6. The analog signal V_{out} is compared with a variable voltage Comp by a fast comparison IC (LM360N) which generates a new digital signal V'_{out}. By calculating the numbers and positions of the pixels with the V'_{out} below 0 V, the spot size and position can be determined and then saved in the CPLD registers. Finally, with the interrupting commands from the computer, data are retrieved from CPLD registers into the computer. Since CCD is sensitive to stray light in the environment in which V_{out} may have unwanted voltage drop. With variable comparison voltage Comp, an adaptive signal V'_{out} can be generated and the tolerance of experiments can be enhanced with this method.

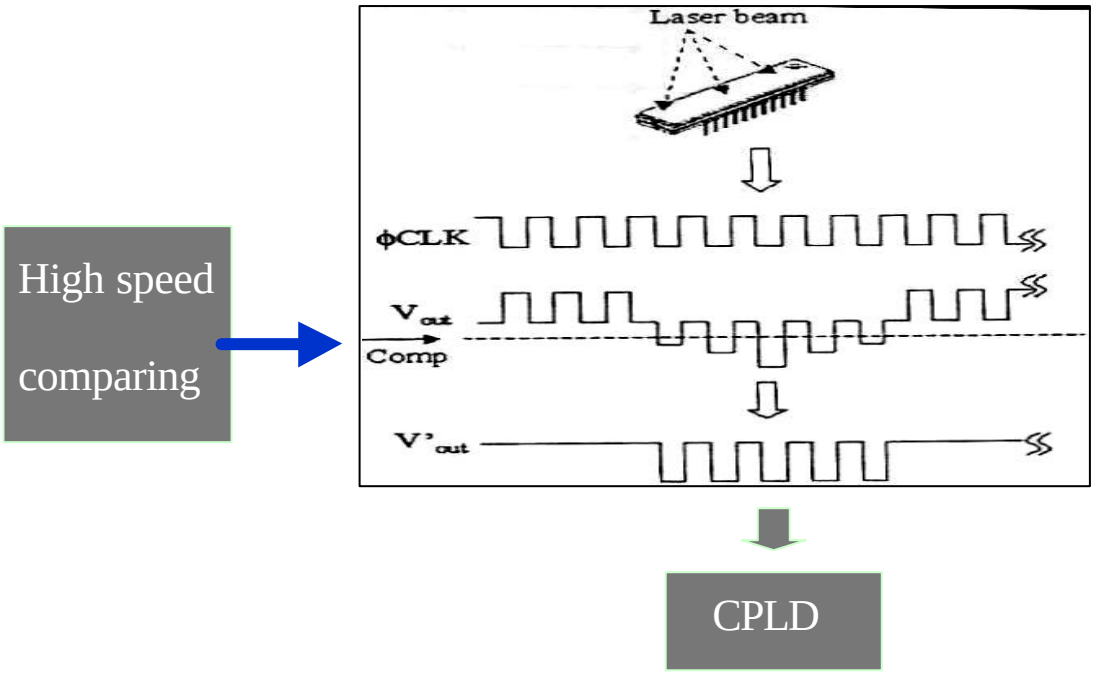

Fig. 3-6 Signal process

3.1.5 Computer Interface

The data saved in the Altera CPLD register can be transferred to the computer with interrupting instructions issued at fixed time intervals. The sequential data contain information about the dynamic features of the mirror.

(1) Arrangement of Altera

The spot sizes and positions are saved separately in the 12-bit registers (counter C and counter P) of CPLD. The driving voltage converted to digital signals by A/D IC is kept in 8-bit register (counter Vin). Since the 4-bit parallel printer port is used to transfer data between the computer and the Altera CPLD, a 8-to-1 multiplexer is added to transfer the 12-bit data, as shown in Fig. 3-7.

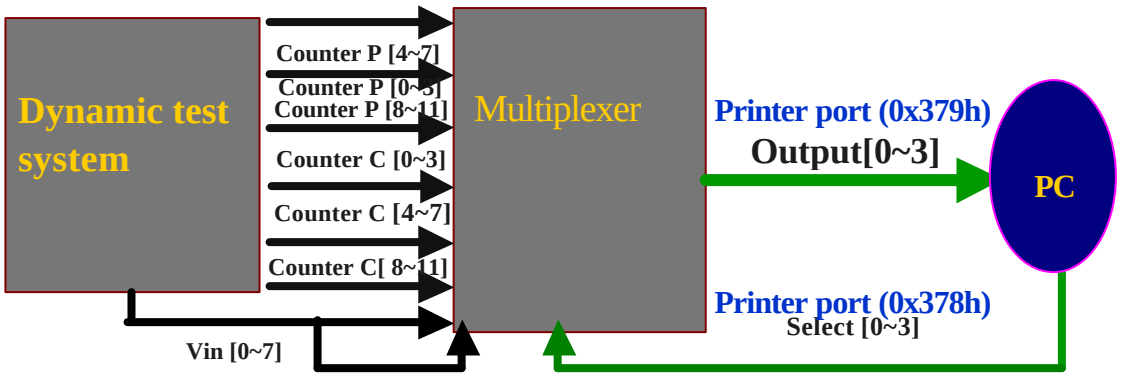

Fig. 3-7 (8 to 1) multiplexer between PC and tester

(2) **Printer port** [20]

The parallel printer port is used for communication between the computer and the measurement system. There are four input bits, eight output bits D0 ~ D7 and other control signals as shown in Fig. 3-8. The interrupting commands generated by the computer is transferred to Altera CPLD through D0~D3 bits and the computer receive the data from multiplexer's output through the four input lines.

0x378h

Output bits:	D7	D6	D5	D4	D3	D2	D1	D0

0x379h

Input bits:	Bu	AC	PE	SLE				

Fig. 3-8 Input and output address of printer port

(3) **Interrupting codes:**

Interruption is one way for the computer to get information from outside. The computer can access outside data at fixed time intervals by using the internal timer. By keeping sending out interrupting instruments every fixed time interval, the computer can obtain the data of CCD tester in synchronization. The design flow of interrupting codes is shown in Fig. 3-9. The data of spot position and size is acquired once through 6 time intervals (recording counter P and counter C) and the data of Vin is obtained through 2 time intervals (recording counter Vin). Each time interval of interrupting system is set to 1ms.

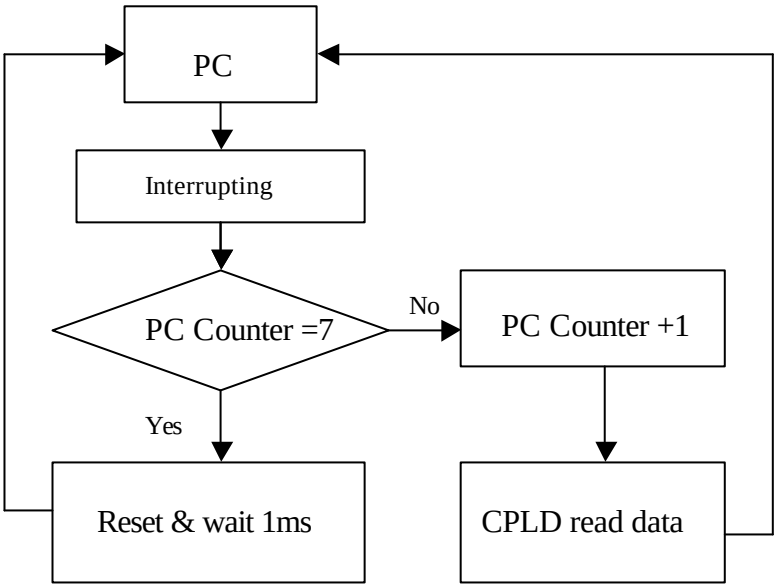

Fig. 3-9 Design flow of interrupting code

3-2 Measurement setup

3.2.1 Setup of CCD measuring system

The circuit diagram of the CCD measurement system is shown in Ref.A-2 and

the simulation of Altera CPLD is also shown in Ref. A-3. The actual optical setup and electronic circuit are shown in Figs. 3-10 and 3-11.

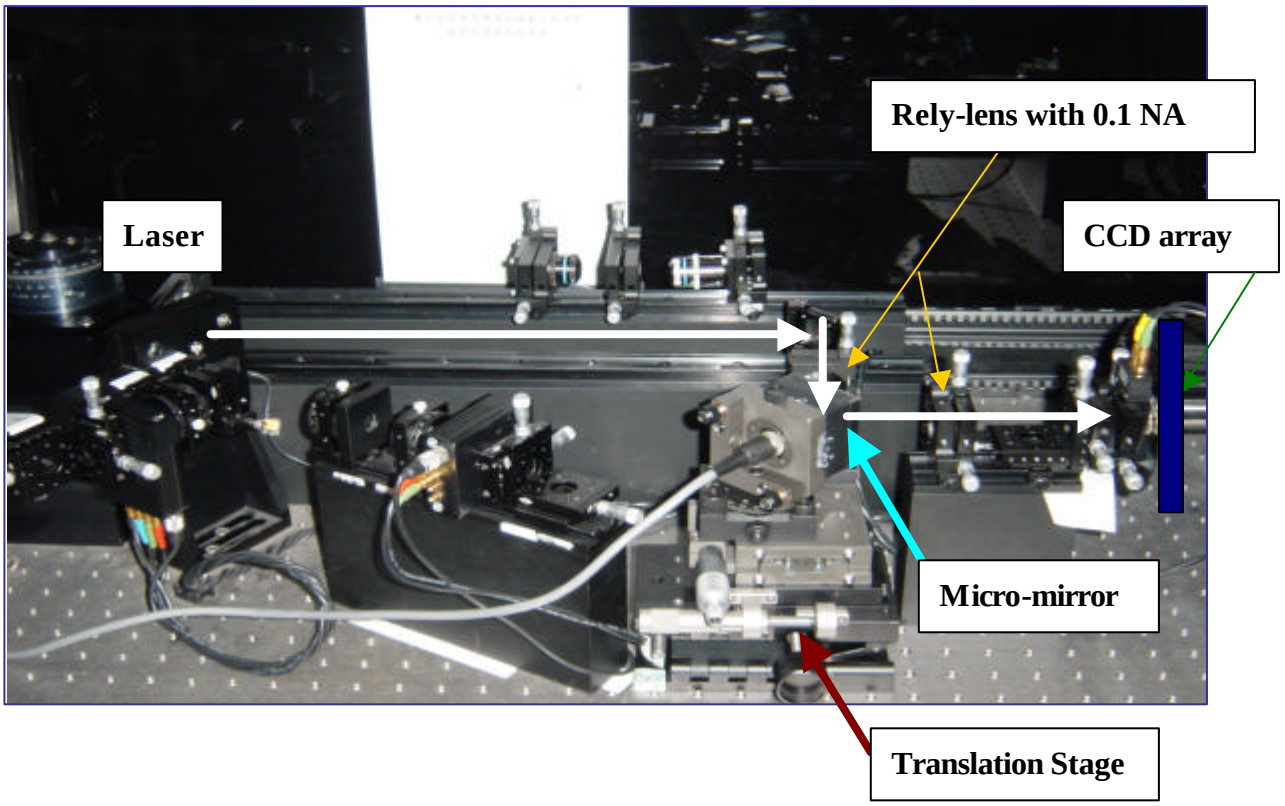

Fig. 3-10 Setup of CCD tester

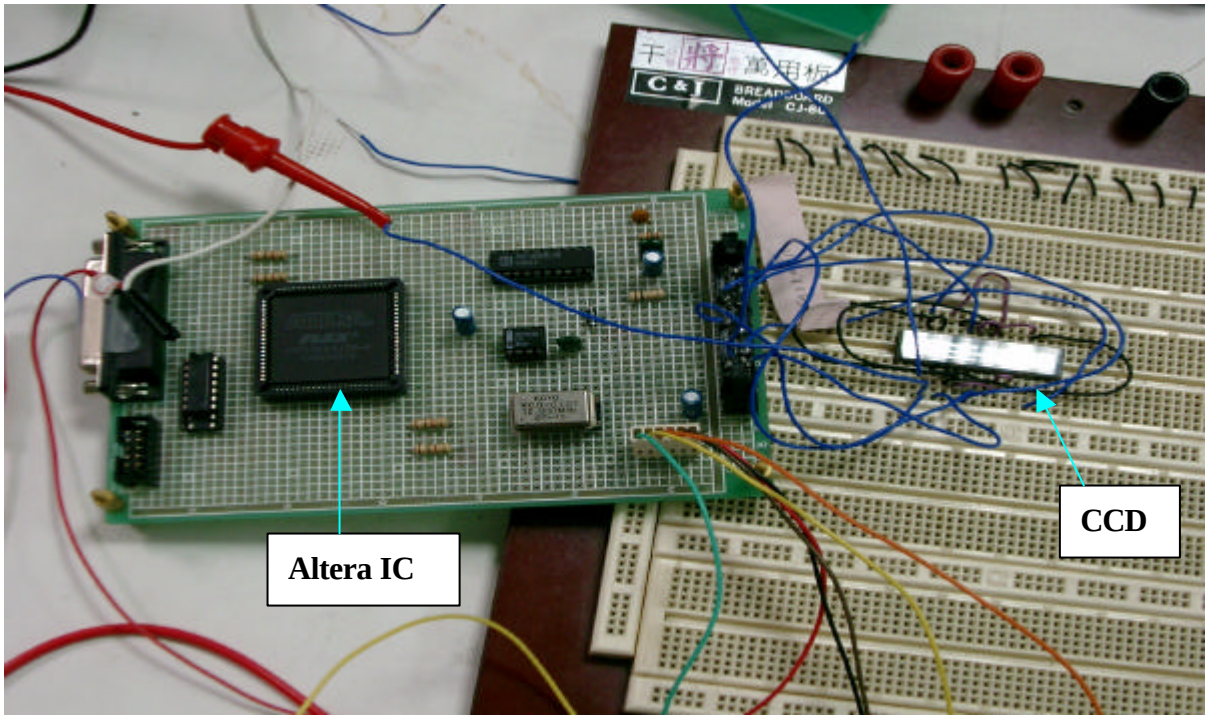

Fig. 3-11 Driving and signal processing circuit

3.2.2 Alignment of the micro-mirror

Light from a laser diode (λ = 0.65 μm) was reflected from the first 45^o mirror and passes through the first focusing rely-lens to the micro-mirror. With the three-axes and two–rotation translation stage, we could adjust the initial angle of micro-mirror to 45 degree as shown in Fig. 3-10. The light reflected from micro-mirror was parallel to the optical axis from laser diode.

3.2.3 Verification of micro-mirror's dynamic features

Before charactering the spot reflected from the micro-mirror, the max operating frequency of CCD needs to be verified. From the specification of CCD, its maximum operating frequency is 5 MHz. As the CCD was driven in 5 MHz, the voltage drop was not clear. It became difficult to adopt appropriate referring voltage for comparing IC generating digital output signals V'_{out} to record spot position and size. Therefore, after several experiments, the operating frequency of CCD is selected to 2 MHz and the scanning frequency of dynamic tester is 976 HZ. (CCD frequency 2 MHz / total pixels 2048)

According to the specification of the micro-mirror, in order to have linear voltage-deflection responses, the driving signals are generated using the following equations:

$$V_1 = V_{bias} + k\,(+V_x - V_y)$$
$$V_2 = V_{bias} + k\,(+V_x + V_y)$$
$$V_3 = V_{bias} + k\,(-V_x + V_y)$$
$$V_4 = V_{bias} + k\,(-V_x - V_y)$$

For the micro-mirror to rotate within horizontal direction X, Vy set to 0V, Vx set to square function from -1.5V to 1.5V and Vbias is set to 50 V. With different operating frequencies, the dynamic features of the micro-mirror can be characterized.

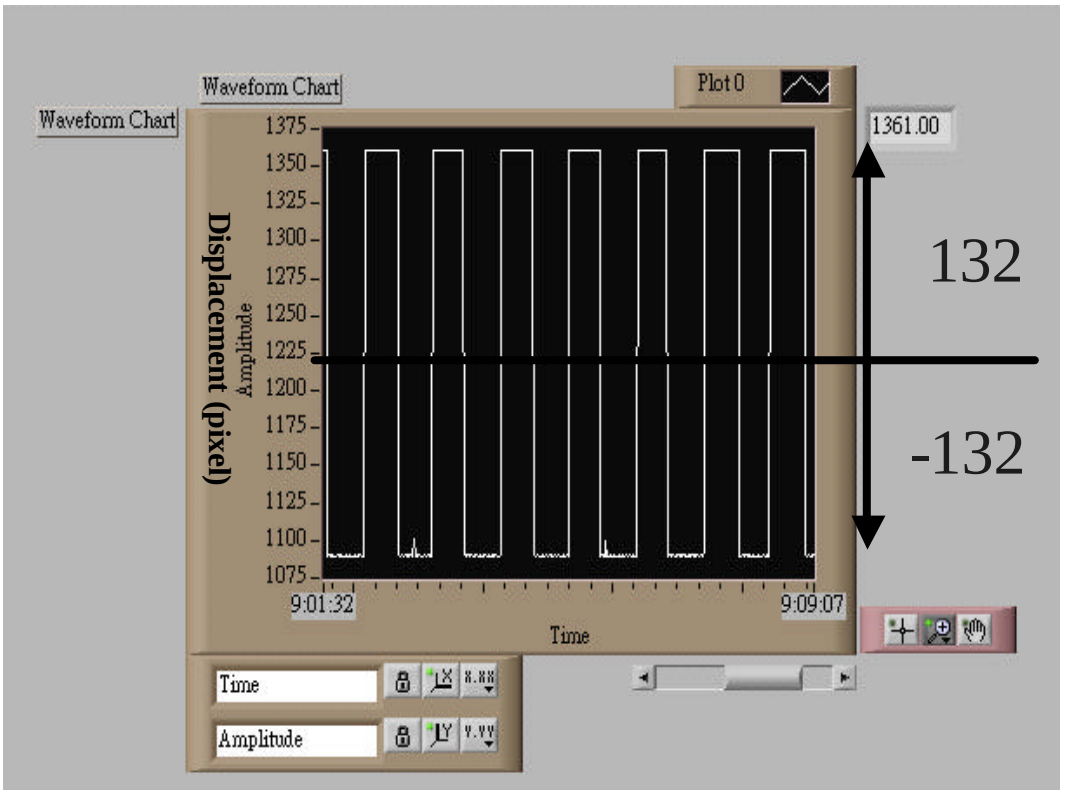

(a) 50 Hz

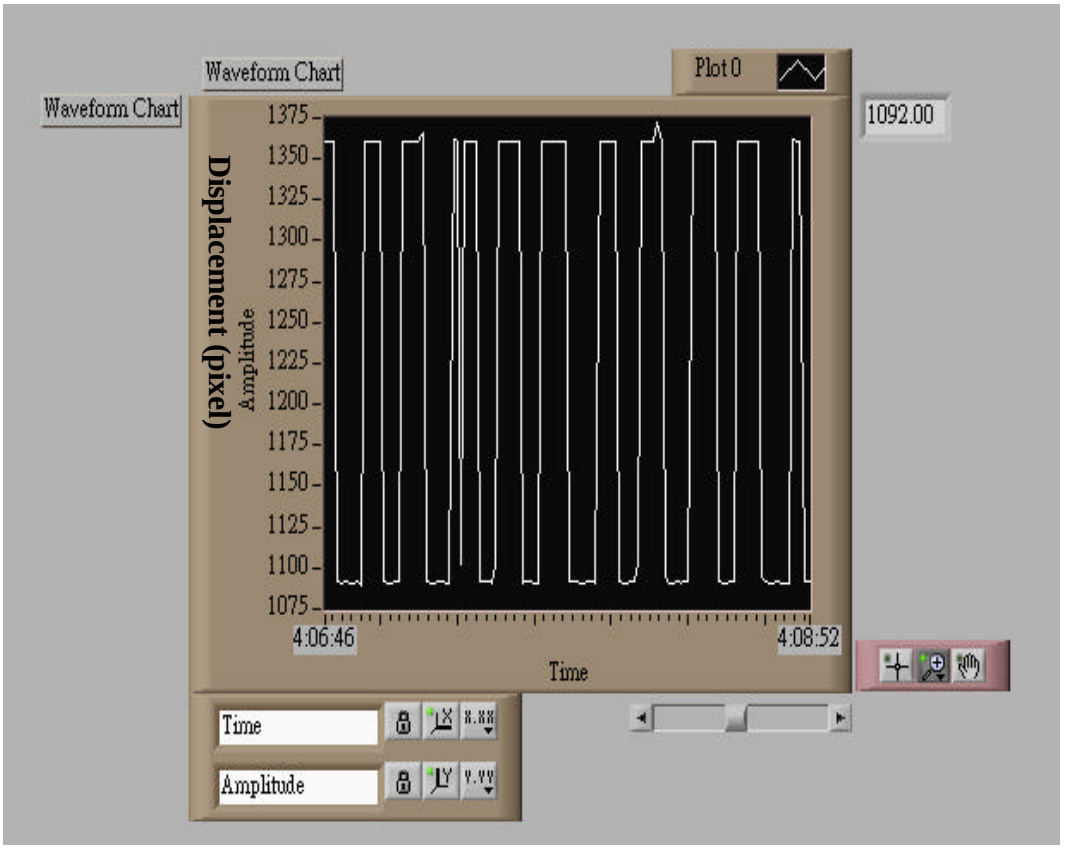

(b) 300 Hz

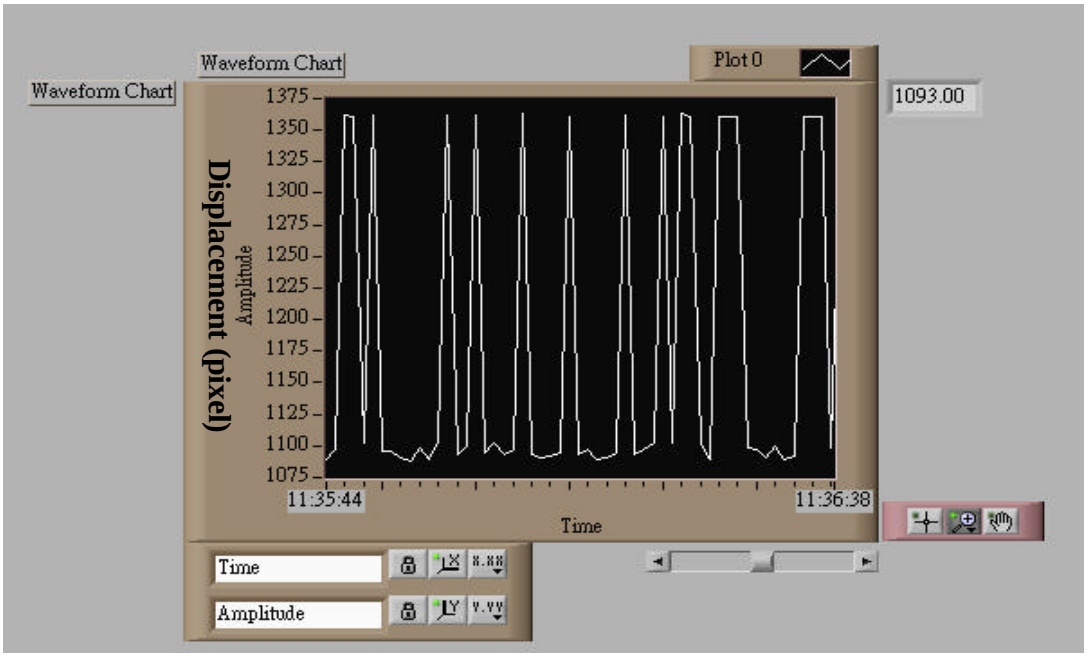

(c) 700 Hz

Fig. 3-12 The spot motion on CCD for driving square function from -1.5V to 1.5V (a) 50 Hz, (b) 300 Hz and (c) 700 Hz

Discussion of experimental results:

(1)**Verification of mirror's tilt angle**

From the results in Fig. 3-12(a), the positive and negative displacement of the spot is 132 pixels, which is equal to 1848 um (one CCD pixel 14um wide). The relation between spot displacement and tilt angle was demonstrated in Fig. 3-13 and Equ. (3-1).

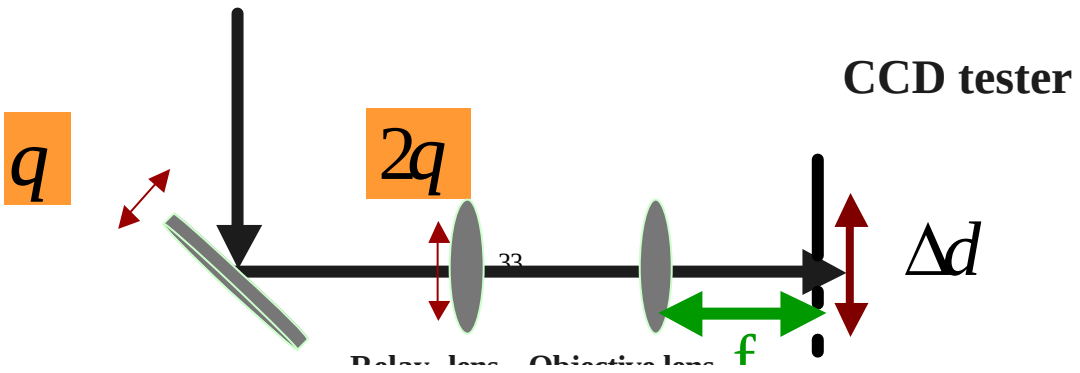

Fig. 3-13 The relation between spot displacement and tilt angle

$$M * 2\Delta q * f = \Delta d \qquad (3\text{-}1)$$

Where M=10 is magnification of relay-lens and objective lens, focus length f = 4 mm and Δd = 1848 um are the focus length of objective lens and the displacement of spot, respectively. Consequently, the mirror's tilt angle Δq was calculated to 1.3 degree, which agrees with the relation between voltage and tilt angle along the Inner Axis from micro-mirror's specification **[15]** as shown in Fig. 3-14. But since the tracking spot displacement of fine tracking actuator such as VCM is defined in ± 500um based on DVD standard; the tilt angle of micro-mirror should be reduced within ± 0.35 degree which results in displacement ± 500 um. The desired tilt angle here is within the tolerated angle ± 1 degree defined in Chapter 2 with maximal tolerated aberration.

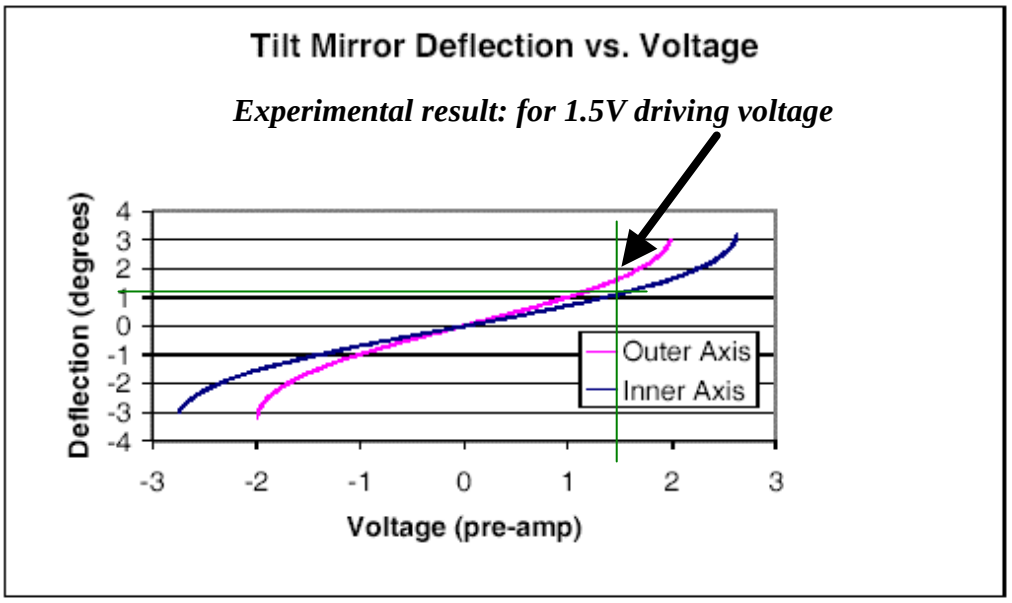

Fig. 3-14 The relation between deflection and voltage by MEMES Optical co.

(2)**Verification of dynamic test**

The experimental results from Fig. 3-12(b) to 3-12(c) show that the measured spot motion due to mirror's tilt is distorted as driven in 300 Hz. With higher driving frequency it is distorted more seriously as shown from Fig. 3-12(a) to 3-12(c). The reason for this phenomenon is that the sampling rate is not enough to describe mirror's feature correctly. The scanning frequency of CCD tester here is 976 Hz (2M Hz/2048 Pixels), where 2 M Hz is the CCD operating frequency and 2048 is the total number of pixels. Therefore, the CCD tester can measure a better waveform by taking more than three sampling points for the actuator driven at less than 300 Hz. If CCD tester's operating frequency could be increased and number of sensing pixels could be reduced, it could be used to measure higher frequency actuator. In order to get correct results and sufficient sensing range, the operating frequency was below 2 MHz and the sensing range was over 2000 pixels. Although CCD tester could not scan enough sampling points for mirror driven over than 300 Hz, it still could measure the static tilt angle of micro-mirror and temporal response of micro-mirror for frequency below 300 Hz. The tilt angle measurement can verify the optical design in tracking system, and temporal response measurement can confirm the identification of physical model.

However, a complete dynamics measurement is still required to identify micro-mirror's physical model. Because the 300 Hz sensing frequency by CCD tester is not enough to identify a complete model for a device that can be driven up to 1k Hz, another experiment is needed to measure the dynamic features of micro-mirror with higher frequency.

3.3 Frequency response measurement

3.3.1 Measurement principle [21]

A photo-detector is used for displacement measurement by sensing the changes of intensity to infer the displacement as shown in Fig. 3-15.

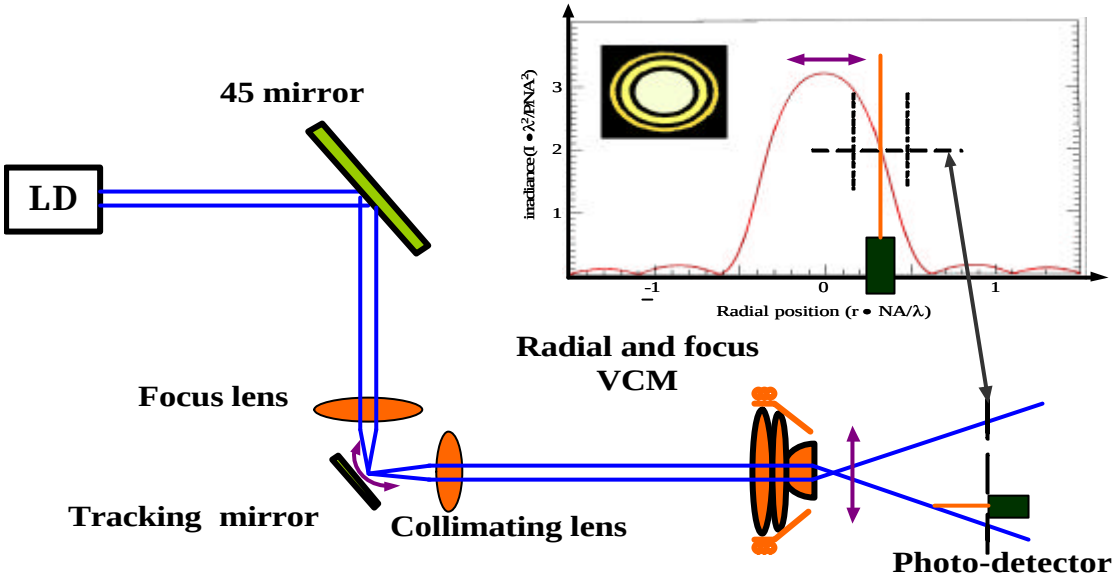

Fig. 3-15 Measurement principle

The linear relation between intensity and the radial position of Gaussian beam is the significant principle used to measure the spot displacement due to mirror's tilt. While we fixed the position of photo-detector but changed the position of the spot, the Gaussian beam would also move with the spot. By sensing the variation of intensity, the displacement of spot could be inferred. This feature results from one linear range between the intensity and radial position in Gaussian separation as shown in Fig. 3-15 above. It is used to judge the displacement of spot by mirror's tilt or actuator's moving.

3.3.2 Measurement set-up

A Dynamic Signal Analyzer (DSA) is used to measure the frequency responses of the radial and focus actuators. Swept Sine is chosen as the excitation signals. The DSA collects the time domain input and output signals of the plant, and gives the frequency response G(jw) in a series of complex numbers.

The method involved for measuring the response of physical system with DSA, such as HP 3562A, is arranged to analyze dynamic features of micro-mirror as shown in Fig. 3-16. The source generated a series of sinusoids with different frequencies to Ch1 and micro-mirror. At the same time, the photo-detector generated the inferred changes of displacements to Ch2. By comparing the measured signals with the driving signals, the frequency response of micro-mirror could be characterized completely by DSA.

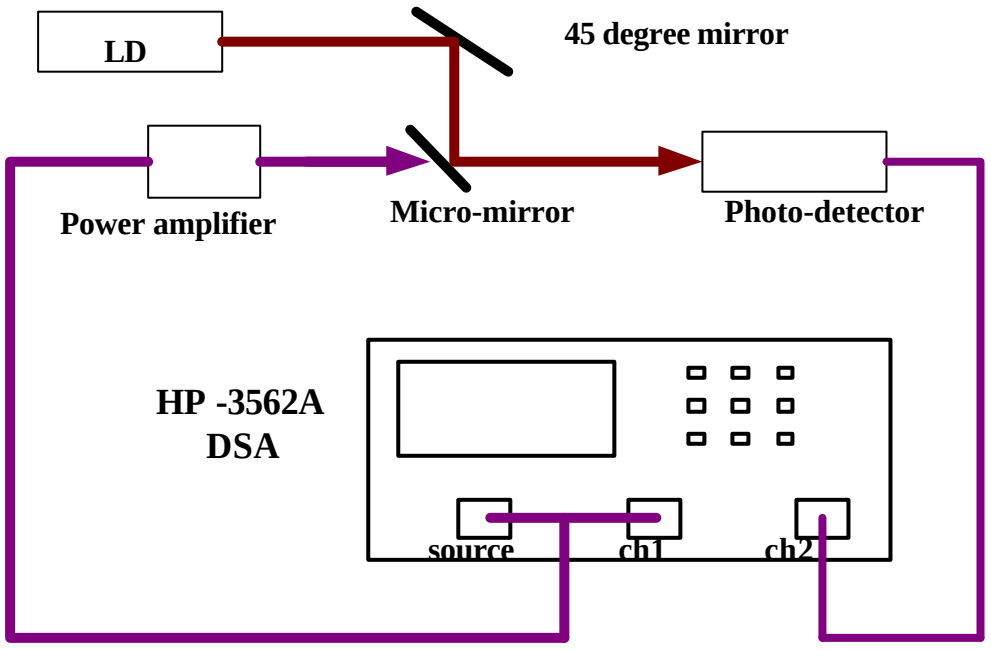

Fig. 3-16 The measurement set-up

3.3.3 Results of micro-mirror's frequency response

The measured frequency response is shown in Fig. 3-17. The first resonance point is at 1.4 kHz. The experimental result is close to the specification of micro-mirror, whose bandwidth is 1.8 k Hz in horizontal direction. We can identify the micro-mirror's transfer function, whose Bode-plot approximates the measured frequency response. Subsequently, a suitable controller can be designed according to the identified physical model as discussed in the next chapter.

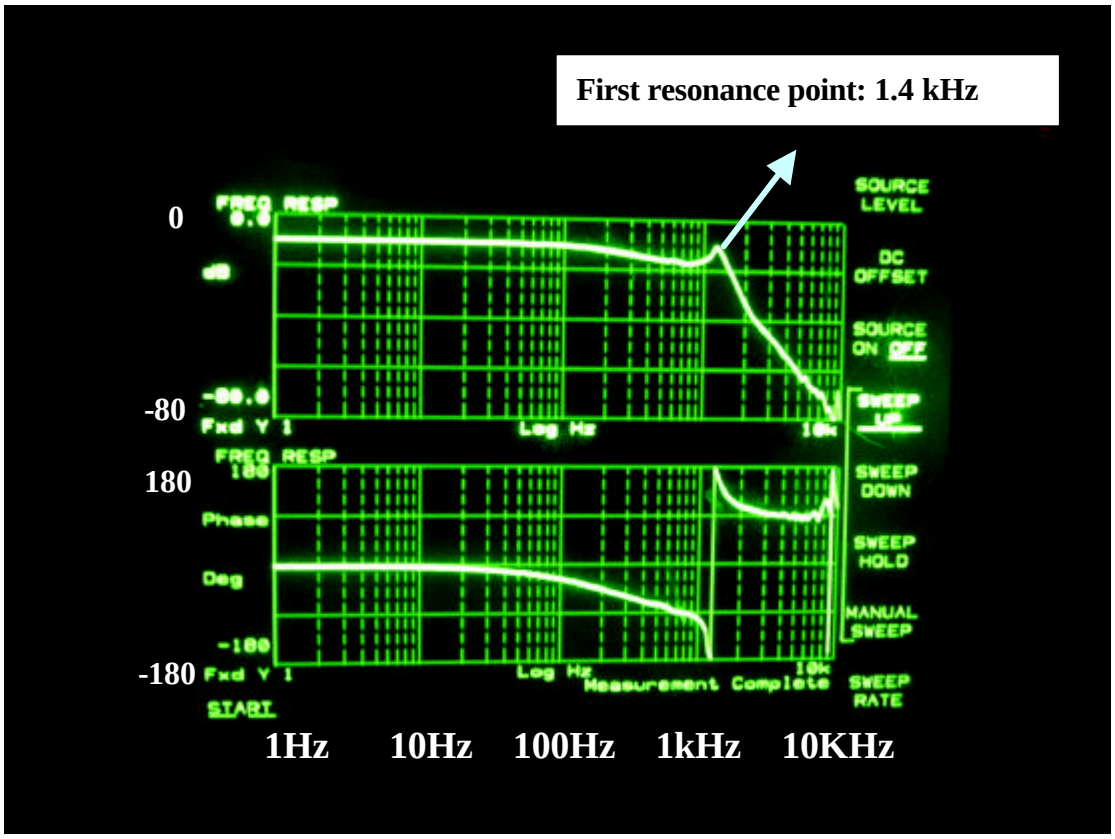

Fig. 3-17 Measured frequency response of micro-mirror